SOLIDWORKS-BASED FINITE ELEMENT MODELING AND SIMULATION OF THE TENSILE AND FLEXURAL STRENGTH OF A 1060-H12 ALUMINUM COMPONENT

Dumbulwa, S.S.*, Yahaya, I. and Abba, U.T.
Department of Mechanical Engineering, Faculty of Engineering, University of Maiduguri, Borno State, Nigeria
*Corresponding email: shuaibudumbulwa08@gmail.com

ABSTRACT

This study applies SolidWorks Simulation to perform a finite element analysis (FEA) of a standard 1060-H12 aluminum rod specimen under static tensile and flexural loading. A three-dimensional model with a reduced gauge section was developed and assigned the linear elastic isotropic properties of 1060-H12 aluminum from the SolidWorks material library (yield strength 57.0 MPa, ultimate tensile strength 85.0 MPa, elastic modulus 69.0 GPa, Poisson's ratio 0.33). A blended curvature-based mesh of 64,159 elements and 93,772 nodes, with 99.9% of elements maintaining an aspect ratio below 3, was generated to ensure solution accuracy. The specimen was subjected to tensile loads of 200 N, 600 N, and 1000 N, as well as concentrated and uniformly distributed flexural loads of the same magnitudes, and the resulting von Mises stress, resultant displacement, and equivalent strain fields were evaluated. Under the maximum 1000 N tensile load, the peak von Mises stress reached 111.4 kPa with a corresponding displacement of 0.000878 mm, while the 1000 N concentrated flexural load produced a substantially higher peak stress of 418.4 kPa with a deflection of 0.00424 mm. In every loading case examined, the induced stresses remained one to three orders of magnitude below the material's 57.0 MPa yield strength, yielding factors of safety well above conventional design thresholds. The results confirm that 1060-H12 aluminum, in the rod geometry studied, is structurally suitable for static, well-defined load regimes and that flexural loading represents the governing design condition relative to axial tension. The study also illustrates the role of SolidWorks Simulation as a validated, CAD-integrated FEA tool for rapid material performance screening ahead of physical prototyping.

Keywords: 1060-H12 aluminum; finite element analysis; SolidWorks Simulation; von Mises stress; tensile loading; flexural loading; factor of safety; mesh convergence

1 INTRODUCTION

Aluminum and its alloys remain among the most widely deployed structural metals in modern engineering because of their favorable strength-to-weight ratio, corrosion resistance, and manufacturability [1, 2]. Within the wrought aluminum families, the 1xxx series is distinguished by very high electrical and thermal conductivity, excellent corrosion resistance, and outstanding cold workability, properties that make it the material of choice for electrical conductors, heat exchangers, chemical process equipment, and general sheet-metal fabrication [3, 4]. As a commercially pure (>99.6% Al) wrought alloy, 1060 derives essentially all of its strength from cold work rather than from precipitation or solid-solution hardening, since it is alloyed with only minor amounts of other elements [3, 5]. The mechanical behavior of 1060 aluminum is therefore governed largely by its temper designation, which records the degree and type of strain hardening applied after rolling. In the Aluminum Association temper system, the suffix H1 denotes strain-hardening alone, and the trailing digit indicates the degree of hardening on a scale that runs from quarter-hard (H12) to full-hard (H18) [3]. The H12 (quarter-hard) condition used in the present study therefore offers a measurable strength increase over the fully annealed (O) condition while retaining substantially more ductility than the harder H14, H16, or H18 tempers; a balance that is frequently exploited in lightweight brackets, spacers, electrical busbars, and similar components where moderate static strength rather than fatigue endurance is the governing design requirement [5]. Reference property compilations report the yield strength of 1060-H12 in the range of roughly 30–61 MPa and the ultimate tensile strength in the range of 70–85 MPa, depending on the exact source and rolling history, with an elastic modulus near 69 GPa and a Poisson's ratio of 0.33 [5, 6, 7]. Computer-Aided Engineering (CAE) tools have become indispensable in translating such material data into predictions of in-service component behavior. Finite element analysis (FEA), the numerical core of most CAE packages, discretizes a continuous structure into a mesh of finite elements over which the governing equations of elasticity are solved approximately, yielding estimates of stress, strain, and displacement fields under prescribed loads and boundary conditions [8, 9]. SolidWorks Simulation, the FEA module embedded within the SolidWorks CAD environment, has been widely adopted in both industry and engineering education because it allows a single parametric solid model to be meshed, loaded, and solved without translation to a separate analysis package, and because benchmark studies coordinated by bodies such as NAFEMS have repeatedly shown its linear static solutions to agree with closed-form analytical results to within about one percent [10, 11]. The same CAD-integrated workflow has been used to optimize gating and runner systems in high-pressure die casting of aluminum alloys [12], to evaluate the structural integrity of precision instrument assemblies under self-weight [13], and to predict the bending response of extruded aluminum structural beams against physical three-point bending tests [14], among many other applications, underscoring its standing as a validated tool for static structural screening ahead of physical prototyping. A central numerical consideration in any FEA study is the quality of the underlying mesh, since the accuracy and stability of the computed stress field depend strongly on element size, shape, and aspect ratio. A mesh convergence study is therefore recognized as essential practice for any FEA exercise intended to support engineering decisions [15, 16]. Closely related is the choice of failure criterion: for ductile metals such as aluminum, the maximum distortion-energy criterion, more commonly known as the von Mises criterion, is the standard basis for predicting the onset of yielding under combined or multiaxial stress states, with yielding assumed to begin once the von Mises equivalent stress reaches the uniaxial yield strength of the material [17, 18]. The ratio of yield strength to von Mises stress at the most highly stressed location then defines the factor of safety, the principal design metric reported throughout the present work. Beyond simple axial tension, structural components made from thin or slender aluminum stock are frequently governed by flexural (bending) loading, in which a transverse force induces a combination of tensile and compressive bending stresses that are typically more severe, for a given load magnitude, than the stress produced by an equivalent axial pull. Three-point and related bending configurations have therefore been used extensively to characterize the flexural response of aluminum sections experimentally and to validate corresponding finite element predictions of deflection and peak bending stress [14, 19]. The distinction between concentrated (point) and distributed transverse loading is likewise of practical importance, since a load spread over a larger contact area reduces local stress concentration relative to an equivalent point load, a relationship long established in classical beam theory and confirmed in numerous finite element comparisons of loading type [17, 20]. Despite the long-standing engineering use of 1060-series aluminum, the published literature contains comparatively few finite element studies that directly quantify its tensile and flexural response side by side under a controlled, mesh-validated CAD-integrated simulation, particularly for the H12 temper. Much of the existing simulation literature on 1000-series aluminum instead addresses forming, casting, or impact behavior [12, 21, 22], leaving a gap with respect to straightforward static structural screening of the kind required by a design engineer selecting stock material for a lightly loaded bracket, rod, or spacer component. The present study addresses this gap. The aim of this work is therefore to use SolidWorks modeling and simulation to investigate, within a single consistent mesh and material framework, the tensile strength and the flexural strength (under both concentrated and distributed transverse loading) of a standard test-specimen geometry made from 1060-H12 aluminum rod, and thereby to establish the load range over which this material and geometry combination can be considered structurally safe for static service.

2 MATERIALS AND METHODS

All modeling and simulation work were carried out in the SolidWorks 2025 design and simulation environment. The material under investigation was 1060-H12 aluminum rod, assigned directly from the SolidWorks material library.

2.1 Geometric Model

A three-dimensional solid model of a standard dog-bone-type test specimen was constructed in SolidWorks. The model incorporated a reduced gauge section at its mid-length, a configuration intended to localize stress concentration and any subsequent failure within the region of interest rather than at the fixture or gripping ends, consistent with conventional tensile-specimen design practice [3].

2.2 Material Properties

The model was assigned the properties of 1060-H12 aluminum rod from the SolidWorks material public library, treated as a linear elastic, isotropic solid. The key mechanical properties used throughout the simulation are summarized in Table 1 and are consistent with independently published property compilations for this temper [5, 6].

2.3 Simulation Setup

Three categories of static structural study were performed in SolidWorks Simulation: (i) Tensile test simulation: one end of the specimen was constrained with a fixed-geometry fixture, and tensile forces of 200 N, 600 N, and 1000 N were applied normal to the opposite end face of the model, in direct tension. (ii) Flexural test simulation — concentrated load: the specimen was supported at both ends with fixed-geometry fixtures, and concentrated point loads of 200 N, 600 N, and 1000 N were applied at the mid-span of the model, replicating a three-point bending configuration [14]. (iii) Flexural test simulation — distributed load: the specimen was again supported at both ends with fixed-geometry fixtures, and the same three load magnitudes (200 N, 600 N, 1000 N) were instead applied as uniformly distributed loads over the central region of the model, allowing the effect of load distribution on peak stress and deflection to be isolated. A blended curvature-based mesh was generated for all simulations using high mesh quality settings, with a minimum of 63,000 elements specified to ensure adequate resolution of the stress field, particularly within the reduced gauge section. Mesh density and quality were assessed using the maximum element aspect ratio and the percentage of elements satisfying an aspect-ratio threshold of less than 3, both widely used indicators of mesh reliability in FEA practice [15]. The resulting mesh statistics are reported in Table 1. For each load case, the solver computed the von Mises equivalent stress, the resultant nodal displacement, and the equivalent strain, and the factor of safety at each load level was subsequently obtained as the ratio of the 57.0 MPa yield strength to the corresponding peak von Mises stress, in line with the maximum von Mises stress failure criterion adopted as the default in SolidWorks Simulation [17, 18].

3 RESULTS AND DISCUSSION

The mesh statistics and material properties used consistently across all nine load cases are presented in Table 1. The mesh comprised 93,772 nodes and 64,159 elements, with a maximum aspect ratio of 4.285 and 99.9% of elements satisfying the aspect-ratio-below-3 criterion generally taken to indicate a numerically reliable mesh [15, 16], supporting confidence that the reported stress and displacement results are not artifacts of poor discretization.

Table 1. Mesh Information and Material Properties of 1060-H12 Aluminum

S/N	Property	Value
1	Total Nodes	93,772
2	Total Elements	64,159
3	Maximum Aspect Ratio	4.285
4	Elements with Aspect Ratio < 3 (%)	99.9
5	Material Designation	1060-H12 Aluminum Rod (SS)
6	Material Model	Linear Elastic Isotropic
7	Failure Criterion	Maximum von Mises Stress
8	Yield Strength	57.0 MPa
9	Ultimate Tensile Strength	85.0 MPa
10	Elastic Modulus	69.0 GPa
11	Poisson's Ratio	0.33
12	Mass Density	2705 kg/m³
13	Shear Modulus	26.0 GPa

Figure 1 shows the resulting solid mesh of the specimen, illustrating the higher element density applied around the gauge-section fillets where stress concentration was anticipated, consistent with standard mesh-refinement practice for regions of expected stress gradients [15].

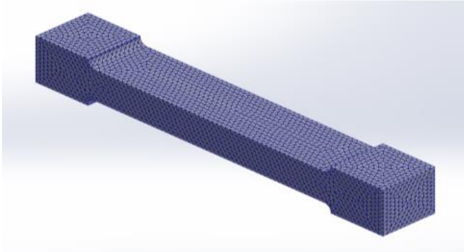

Figure 1. Meshed model of the 1060-H12 aluminum specimen, showing the blended curvature-based mesh refined within the reduced gauge section

3.1 Tensile Loading Analysis

The specimen was subjected to axial tensile loads with one end fixed and the load applied normal to the opposite face. At a 200 N load, Figure 2 shows the resulting tensile stress distribution, with a maximum von Mises stress of 22.29 kPa concentrated at the gauge-section fillet, while Figure 3 shows the corresponding displacement field, with a maximum resultant displacement of 0.000176 mm at the loaded end.

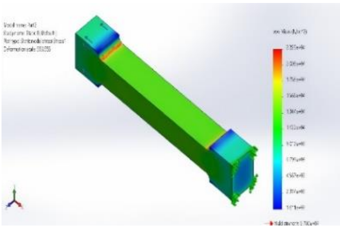

Figure 2. Tensile stress due to 200 N load

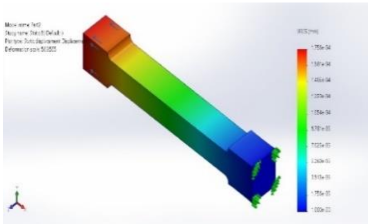

Figure 3. Tensile displacement due to 200 N load

Increasing the load to 600 N produced a proportional rise in the peak stress to 66.86 kPa (Figure 4), with the corresponding maximum displacement, shown in Figure 5, reaching 0.000527 mm.

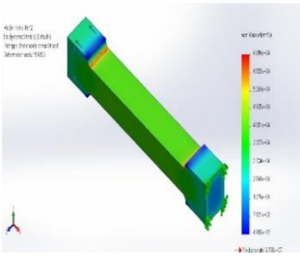

Figure 4. Tensile stress due to 600 N load

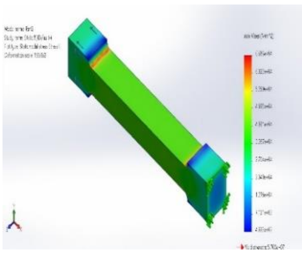

Figure 5. Tensile displacement due to 600 N load

At the maximum tensile load of 1000 N, Figure 6 shows the specimen reaching a peak von Mises stress of 111.4 kPa, with the corresponding maximum displacement of 0.000878 mm presented in Figure 7.

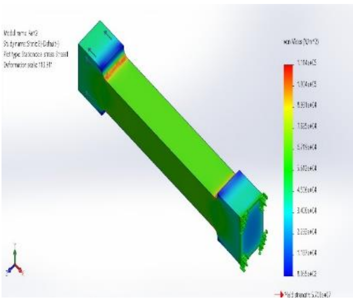

Figure 6. Tensile stress due to 1000 N load.

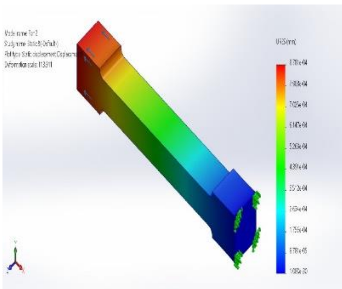

Figure 7. Tensile displacement due to 1000 N load.

Across all three tensile load cases, the induced von Mises stresses (22.29–111.4 kPa) remained more than two orders of magnitude below the 57.0 MPa yield strength of 1060-H12 aluminum, and the resulting factors of safety indicate that axial tension within this load range poses essentially no risk of yielding for the geometry studied. This behavior is consistent with the expectation that a slender rod loaded purely in axial tension develops comparatively low and uniform stress across its cross-section, in contrast to the localized bending stresses examined next.

3.2 Flexural Loading Analysis

The specimen was next subjected to flexural (bending) loads with both ends supported by fixed-geometry fixtures, under both concentrated (point) and uniformly distributed loading conditions, to evaluate the influence of load distribution on the resulting stress and deflection.

3.2.1 Concentrated (point) flexural load

Under a 200 N concentrated mid-span load, Figure 8 shows a maximum flexural stress of 83.69 kPa, while Figure 9 shows the corresponding maximum deflection of 0.000849 mm.

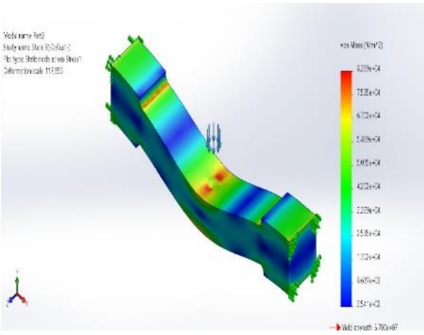

Figure 8. Flexural stress due to a concentrated 200N load

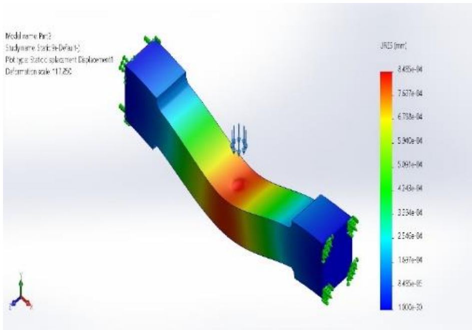

Figure 9. Deflection due to a concentrated 200N load

At 600 N, the peak stress, shown in Figure 10, rose to 251.1 kPa, with the deflection illustrated in Figure 11 increasing to 0.00255 mm.

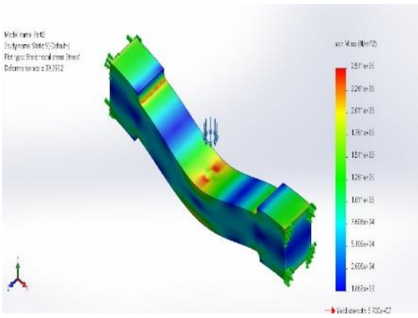

Figure 10. Flexural stress due to a concentrated 600N load

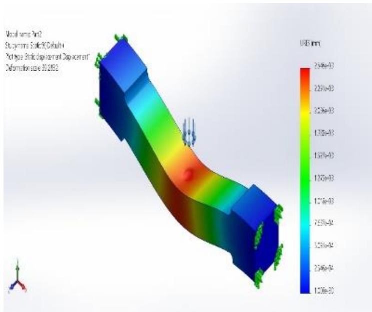

Figure 11. Deflection due to a concentrated 600N load

At the maximum concentrated load of 1000 N, Figure 12 shows the stress distribution reaching 418.4 kPa, with the resulting deflection of 0.00424 mm shown in Figure 13.

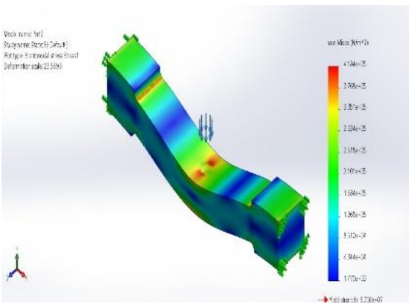

Figure 12. Flexural stress due to a concentrated 1000N load

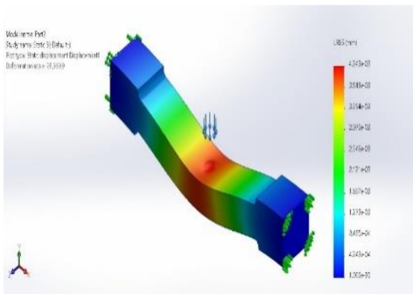

Figure 13. Deflection due to a concentrated 1000N load

3.2.2 Distributed flexural load

Under an equivalent 200 N load applied as a uniformly distributed load, Figure 14 shows a maximum stress of 71.76 kPa, with the corresponding maximum deflection of 0.000536 mm presented in Figure 15.

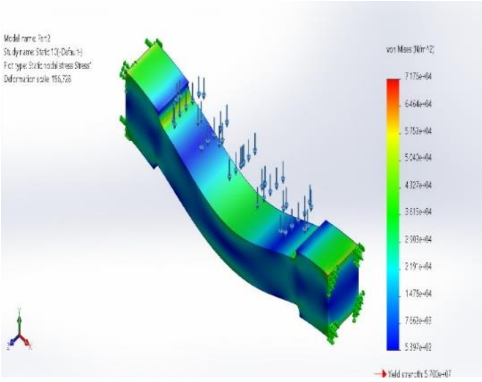

Figure 14. Flexural stress due to a distributed 200N load

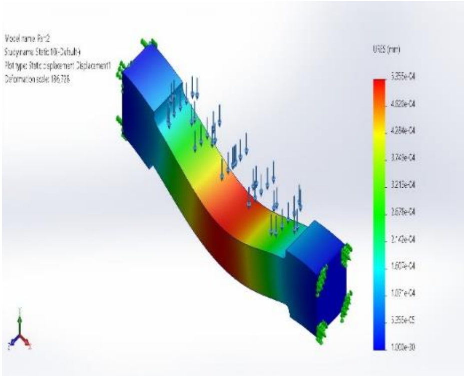

Figure 15. Deflection due to a distributed 200N load

At 600 N, the maximum stress shown in Figure 16 reached 215.3 kPa, with the corresponding deflection, presented in Figure 17, equal to 0.00161 mm.

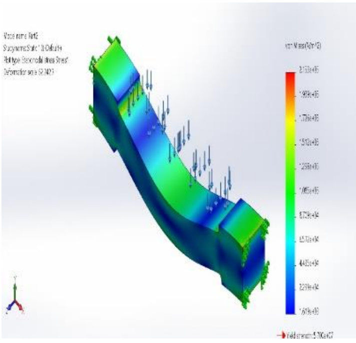

Figure 16. Flexural stress due to a distributed 600N load

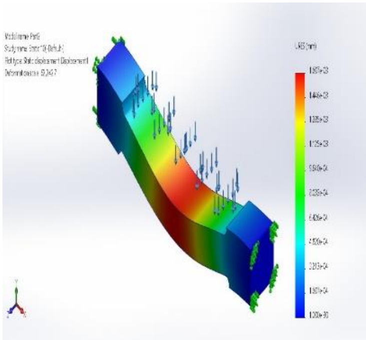

Figure 17. Deflection due to a distributed 600N load

At the maximum distributed load of 1000 N, Figure 18 shows the stress reaching 358.8 kPa, with the corresponding deflection of 0.00268 mm shown in Figure 19.

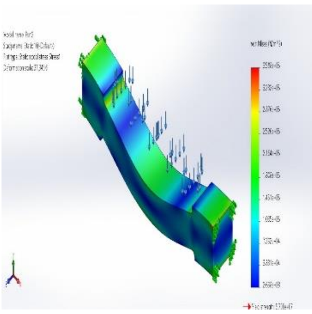

Figure 18. Flexural stress due to a distributed 1000N load

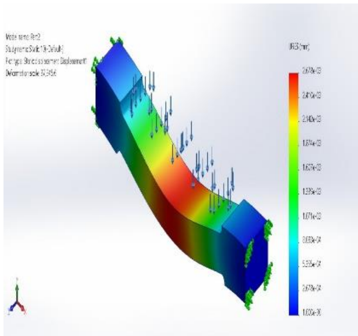

Figure 19. Deflection due to a distributed 1000N load

As expected from classical beam theory, the concentrated loads generated consistently higher peak stresses and deflections than the equivalent distributed loads at every load magnitude examined for instance, 418.4 kPa versus 358.8 kPa at 1000 N, and 83.69 kPa versus 71.76 kPa at 200 N because the same total force is delivered over a smaller effective area in the concentrated case, producing a sharper local stress gradient [17, 20]. This pattern was consistent across all three load levels, confirming that load distribution exerts a measurable and predictable influence on the severity of flexural stress for a fixed total applied force. Comparing loading modes overall, flexural loading produced substantially higher stresses than axial tension for an equivalent applied force: at 1000 N, the concentrated flexural stress of 418.4 kPa was approximately 3.8 times the 111.4 kPa tensile stress, despite both cases sharing the same 1000 N load magnitude and the same material and mesh. This is consistent with the well-established mechanics of bending, in which the bending moment generated by a transverse load produces stress that is amplified by the specimen's slenderness, in contrast to the comparatively uniform stress field developed under direct axial tension [17]. Flexural loading therefore represents the more critical design condition for this geometry and should govern any safety assessment where both loading modes are plausible in service. Despite this amplification, all recorded flexural stresses (71.76–418.4 kPa) remained well below the 57.0 MPa yield strength of 1060-H12 aluminum, corresponding to factors of safety ranging from approximately 136 (concentrated, 1000 N) to nearly 800 (distributed, 200 N), as summarized in Table 2. Even under the most severe loading condition examined — the 1000 N concentrated flexural load — the component retained a substantial safety margin, and the associated deflections (a maximum of 0.00424 mm) were negligible relative to the specimen's overall dimensions, indicating high structural stiffness for this geometry and material combination.

Table 2. Summary of Maximum von Mises Stress, Displacement, and Factor of Safety Across All Load Cases

Load Type	Load (N)	Max. von Mises Stress (kPa)	Max. Displacement / Deflection (mm)	Factor of Safety*
Tensile	200	22.29	0.000176	2557
Tensile	600	66.86	0.000527	852
Tensile	1000	111.4	0.000878	512
Flexural – concentrated	200	83.69	0.000849	681
Flexural – concentrated	600	251.1	0.00255	227
Flexural – concentrated	1000	418.4	0.00424	136
Flexural – distributed	200	71.76	0.000536	794
Flexural – distributed	600	215.3	0.00161	265
Flexural – distributed	1000	358.8	0.00268	159

**Factor of safety calculated as yield strength (57.0 MPa) divided by the maximum von Mises stress recorded for each case.*

4 CONCLUSIONS

This study used SolidWorks modeling and simulation to investigate, within a single mesh-validated finite element framework, the tensile and flexural performance of a standard 1060-H12 aluminum rod specimen under static loads of up to 1000 N. The component withstood all tensile, concentrated-flexural, and distributed-flexural load cases examined without approaching its 57.0 MPa yield strength, recording a maximum von Mises stress of 111.4 kPa in tension and 418.4 kPa in concentrated flexure — factors of safety of approximately 512 and 136, respectively, at the highest load level tested. Flexural loading consistently produced higher stresses than equivalent axial tension, and concentrated transverse loads consistently produced higher stresses and deflections than equivalent distributed loads, identifying concentrated flexural loading as the governing design condition for this geometry. All recorded deformations were negligible (no greater than 0.00424 mm), confirming high structural stiffness for the specimen geometry investigated. Taken together, the results indicate that 1060-H12 aluminum rod, in the configuration studied, is structurally suitable for static engineering applications with well-defined, moderate load profiles, and the study provides a validated reference point for lightweight design decisions involving this material. Future work could usefully extend the present static analysis to fatigue loading, to experimental validation by physical tensile and bending testing, and to a broader range of specimen geometries and support conditions.

REFERENCES

1. Okokpujie, I.P., Chima, P.C. and Tartibu, L.K. (2021). Experimental and 3D-Deform finite element analysis on tool wear during turning of Al-Si-Mg alloy, *Heliyon*, vol. 7, no. 10, e08106.

2. Yang, Y., Zhao, Q. and Liu, X. (2021). Microstructure, texture and mechanical properties of AA 1060 aluminum alloy processed by cryogenic accumulative roll bonding, *Materials Science and Engineering: A*, vol. 822, 141680.

3. Davis, J.R. (2001). Aluminum and Aluminum Alloys. ASM Specialty Handbook. Materials Park, OH: *ASM International*.
4. Azo, M. (2013). Aluminium / Aluminum 1060 Alloy (UNS A91060). *AZoM Materials Database*, 11 June 2013. Available at: https://www.azom.com/article.aspx?ArticleID=6587.
5. MakeItFrom (2020). 1060-H12 Aluminum. Available at: https://www.makeitfrom.com/material-properties/1060-H12-Aluminum.
6. MatWeb (2024). Aluminum 1060-H12. *MatWeb Material Property Data*. Available at: https://www.matweb.com.
7. BeamDimensions (2024). 1060-H12 Material Properties: Aluminum Properties, Yield Strength, Aluminum Specifications. Available at: https://beamdimensions.com/materials/Aluminium/CSA_S157/1060-H12/.
8. Zienkiewicz, O.C. and Zhu, J.Z. (1987). A simple error estimator and adaptive procedure for practical engineering analysis, *International Journal for Numerical Methods in Engineering*, vol. 24, no. 2, pp. 337-357.
9. Felippa, C.A. (2004). Introduction to Finite Element Methods. Boulder, CO: University of Colorado Lecture Notes.
10. SolidWorks (2024). SOLIDWORKS Simulation | Structural Analysis Software. Dassault Systèmes. Available at: https://www.solidworks.com/product/solidworks-simulation.
11. Hawk Ridge Systems (2023). SOLIDWORKS Simulation – Accurate Finite Element Analysis (FEA) Software. Available at: https://hawkridgesys.com/solidworks-simulation.
12. El Mehtedi, M., Mancia, T., Buonadonna, P., Guzzini, L., Santini, E. and Forcellese, A. (2020). Design optimization of gate system on high pressure die casting of AlSi13Fe alloy by means of finite element simulations, *Procedia CIRP*, vol. 88, pp. 509-514.
13. Riley, A., Larkin, K., Chiang, F. and Wright, S.A. (2024). Liger at W.M. Keck Observatory: imager structural analysis, fabrication, and characterization plan, *arXiv preprint*, arXiv:2409.16263.
14. Chen, B.C., Chiang, W.R., Lee, Y.C. and Chang, Y.C. (2020). Experiment and finite element analysis study on the deflection of aluminum extruded 6063-T5 hollow structural beam, *IOP Conference Series: Materials Science and Engineering*, vol. 711, 012075.
15. Logesh, K. (2020). Mesh convergence study and estimation of discretization error of hub in clutch disc with integration of ANSYS, *IOP Conference Series: Materials Science and Engineering*, vol. 402, 012065.
16. Burkhart, T.A., Andrews, D.M. and Dunning, C.E. (2013). Finite element modeling mesh quality, energy balance and validation methods: a review with recommendations associated with the modeling of bone tissue, *Journal of Biomechanics*, vol. 46, no. 9, pp. 1477-1488.
17. Hibbeler, R.C. (2017). Mechanics of Materials. 10^{th} edn. *Boston: Pearson*.
18. Ansys (2023). What Is Equivalent Stress? *Ansys Knowledge Resources*. Available at: https://www.ansys.com/blog/what-is-equivalent-stress.
19. Belingardi, G., Beyene, A.T. and Koricho, E.G. (2018). Bending performance and energy absorption of aluminium and composite beams: an experimental and numerical study, *International Journal of Crashworthiness*, vol. 23, no. 4, pp. 381-395.
20. Liu, Y., Zhang, X. and Wang, H. (2023). Comparative finite element study of concentrated and distributed loading effects on beam-type structural components, *Mechanics & Industry*, vol. 24, pp. 1-12.

21. Wang, J., Zhang, K. and Li, Y. (2018). Damage and failure analysis of 1060 aluminum sheet under low-velocity impact using finite element simulation, *International Journal of Impact Engineering*, vol. 118, pp. 30-41.

22. Zhao, L., Sun, H. and Feng, P. (2022). Natural frequency analysis of a 1060 aluminum alloy mixer structure using finite element analysis, *Journal of Vibroengineering*, vol. 24, no. 3, pp. 512-523.

23. Mohiuddin, M.V., Krishnaiah, A. and Hussainy, S.F. (2015). Influence of sand molding process parameters on product quality of Al-Si alloy casting – an ANOVA approach, *International Journal of Advance Research in Science and Engineering*, vol. 4, issue 1.

24. Rathinam, N., Dhinakaran, R. and Sharath, E. (2021). Optimizing process parameters to reduce blowholes in high pressure die casting using Taguchi methodology, *Materials Today: Proceedings*, vol. 38, part 5, pp. 2871-2877.

25. Tariq, S., Tariq, A., Masud, M. and Rehman, Z. (2022). Minimizing the casting defects in high-pressure die casting using Taguchi analysis, *Scientia Iranica B*, vol. 29, no. 1, pp. 53-69.

26. Thirugnanam, M. (2013). Modern high-pressure die-casting processes for aluminum castings, *Transactions of the 61st Indian Foundry Congress*, pp. 1-7.

27. Ubani, N.O. (2023). *Mechanical behaviour of aluminium alloys under static loading*. Department of Mechanical Engineering, Chukwuemeka Odumegwu Ojukwu University, Uli.